Revista de la Construcción
ISSN: 0717-7925
revistadelaconstruccion@uc.cl
Pontificia Universidad Católica de Chile
Chile

Rivera, Jhonathan F.; Mejia, Johanna M.; Mejia de Gutierrez, Ruby; Gordillo, Marisol
Hybrid cement based on the alkali activation of by-products of coal
Revista de la Construcción, vol. 13, núm. 2, agosto, 2014, pp. 31-39
Pontificia Universidad Católica de Chile
Santiago, Chile

Hybrid cement based on the alkali activation of by-products of coal

Cementos híbridos basados en la activación alcalina de subproductos del carbón

Jhonathan F. Rivera (Main Author)
School of Materials Engineering, Composite Materials Group (GMC, CENM), Universidad del Valle. Cali, Colombia
jhonathan.rivera@correounivalle.edu.co / jhorivkan@hotmail.com
Fono/fax (57-2-3302436), Calle 13 #100-00 Edificio 349, 2° piso, Cali, Colombia

Johanna M. Mejia
GMC, Universidad del Valle/Colombia
johanna.mejia@correounivalle.edu.co

Ruby Mejia de Gutierrez (Contact Author)
GMC, Universidad del Valle/Colombia
ruby.mejia@correounivalle.edu.co

Marisol Gordillo
GMC, Universidad Autónoma de Occidente/Cali, Colombia
mgordillo@uao.edu.co

Manuscript Code: 0291
Date of reception/acceptation: 01jan2014/01aug2014

Resumen
Este estudio se propuso la producción de un material cementicio alternativo de bajo impacto ambiental a partir de la evaluación de dos subproductos de la combustión del carbón. Se elaboraron dos cementos híbridos basados en la activación alcalina de una ceniza volante (FA) y una escoria de parrilla (BS) y adicionados con cemento portland (OPC) hasta en un 30%. FA y BS contienen hasta un 16% de inquemados. Para la optimización de la resistencia a la compresión se utilizó la Metodología de Superficie de Respuesta (MSR). El geopolímero BS alcanzo alta resistencia a la compresión (>100 MPa a 28 días) y el geopolímero FA reporto 30 MPa al aplicar curado térmico. La adición de OPC contribuyo a modificar el método de curado. En el caso del hibrido basado en FA (HFA), se observó un incremento significativo en la resistencia a niveles hasta de 65 MPa a 28 días sin aplicar el curado térmico.

Palabras claves: Cemento híbrido, ceniza volante, escoria de parrilla, materiales activados alcalinamente, baja huella de carbono.

Abstract
This study focuses on the production of an alternative cementitious material with low environmental impact through the evaluation of two-coal combustion by-products. Hybrid cements based on the alkali activation of fly ash, (FA) and boiler slag (BS) blend with a proportion of Portland cement (OPC) up to 30% were produced. FA and BS contain an unburned material up to 16%. Response Surface Methodology (RSM) was used to optimize the compressive strength. BS geopolymer achieved high compressive strength (>100 MPa at 28 days) and FA geopolymer reached 30 MPa with thermal curing. The addition of OPC helped modify the curing method. In the case of hybrid based on FA (HFA), there was a significant increase in the compressive strength with levels ranging up to 65 MPa at 28 days without requiring a thermal curing.

Keywords: Hybrid binder, fly ash, boiler slag, alkali-activated materials, low carbon footprint.

Introduction

The report N° 9 (November 6th 2013) of the World Meteorological Organization shows that the atmospheric CO_2 concentration between 2011 and 2012 was higher than the average of the last ten years. The United States and China, followed by the European Union and India, are considered the world's largest emitters; this is associated with industrialization, economic development and the ever-increasing opening of coal-fired power plants (in China, coal represents 68% of the country's energy consumption). Concrete is the second most used material in the planet after water, and since China accounts for 58% of the world's cement production (4.0 billion tons in 2013) (Van Oss, 2014), the increase in CO_2 emissions is also attributed to the production of this material. The emissions are due both to the use of limestone as raw material and of fossil fuels to reach the required temperatures for the clinkering process. For this reason, the Portland cement (OPC) industry has been considered responsible for approximately 6-8% of the global anthropogenic CO_2 emissions (Yoon et al., 2014; Damtoft et al., 2008).

Solutions put forward include increasing energy efficiency, the use of alternative fuels, substitution of raw materials by other non-carbonated sources and the partial substitution of cement with supplementary materials (SCM), such as pozzolans and blast furnace steel slags, among others (Lothenbach et al., 2011; Imbabi et al., 2012; Díaz et al., 2013; Robayo et al., 2013). Another option is the development of cements that, keeping at least the characteristics of current cements, require less energy to manufacture and/or use other types of raw materials, therefore offering greater technical and environmental sustainability (Schneider et al., 2011). As a result, alkali-activated cements, geopolymers and more recently hybrid cements which are alkali-activated cements with less than 30% of Portland cement clinker have emerged (Fernández-Jimenez et al., 2011; Palomo et al., 2007; Shi et al., 2011). These cements also being included in the category of the *Potential Low Carbon Cements*.

Hybrid cements aim to combine the positive characteristics of the traditional OPC materials with those of the alkali-activated materials, generating new materials with higher durability and mechanical properties due to the coexistence of the hydration products a mixture of calcium silicate hydrate (C-S-H) and aluminosilicate or geopolymer (N-A-S-H) gels (Cabrera-Fuentes et al., 2011; García-Lodeiro et al., 2009). To date, laboratory studies have demonstrated that in the presence of Ca and at high pH, the precipitation of C-S-H or C-A-S-H is guaranteed, whereas at a pH lower than 11.5 the presence of calcium is not aggressive enough to degrade the N-A-S-H gel and allow for ion exchange with Na+. On the contrary, this can produce a gel able to adsorb the calcium present leading to 3D type structures of (N,C)-A-S-H (García-Lodeiro et al., 2013; Macphee & García-Lodeiro, 2011). One category of these new Hybrid cements are the alkali-activated Portland blended cements; here, adding the alkaline activators can increase the pozzolanic potential, allowing the

use of large quantities of pozzolans or of lower quality materials (Shi et al., 2011).

This article presents a comprehensive overview of the compressive strength up to 90 days of curing of two hybrid binders synthesized from coal combustion wastes: BS, coming from an industrial boiler and FA, generated in a Colombian thermal power plant. These by-products present a high level of unburned carbon and a reduced proportion of amorphous material; their physical and chemical characteristics are directly linked to the processing method: coal particle size, combustion variables, cooling method and collecting process. Other properties such as chloride permeability and electrical resistivity of the samples were also evaluated. Additionally, the microstructural characterization of the geopolymers was conducted, using FTIR and DRX techniques.

Experimental methodology

Materials

The experiments run in this study were conducted on two coal by-products used as geopolymer precursors: fly ash (FA), sourced from a Colombian thermal power plant (Termopaipa GENSA) and boiler slag (BS), from an industrial site. The chemical composition of these two materials, as shown in Table 1, corresponds to aluminosilicates. Their high content of unburned residues should be highlighted; it exceeds the maximum recommended level in the Standard ASTM C618 for use as pozzolanic material. The source of calcium used in the production of the hybrid binder was OPC; its chemical composition, included in Table 1, shows that it corresponds to a blended cement with limestone.

Table 1. *Chemical composition (%wt) (LOI is loss on ignition at 1000°C). (Source: Self-Elaboration)*

Materials	SiO_2	Al_2O_3	*CaO*	Fe_2O_3	*MgO*	*LOI*
BS	48.10	24.80	0.76	7.48	0.53	16.00
FA	53.73	21.54	0.78	4.47	0.56	14.68
OPC	20.20	7.00	58.40	4.80	-	9.60

Although FA and BS are both coal combustion by-products, their morphology particle size and texture differs due to their different processing method. The microstructural observations by SEM show that FA's particles are spherical whereas BS' are irregular and angular (Figure 1). This is attributed to the fact that fly ash is produced by the fusion of small and light particles that remain suspended in the burning chamber and are captured afterwards by electrostatic filtration equipment whereas boiler slag goes through a fusion and agglomeration process in the bottom of the boiler where the coal is burned. FA presented an average particle size of 63.9 µm and BS of 50 mm approximately. FA was grinded in a ball mill during 90 minutes in order to reach a particle size of 19 µm. After a preliminary grinding in a disc mill, BS was grinded in a ball mill during 120 minutes in order to obtain the same average particle size.

X-Ray diffractograms of the materials used are also presented in Figure 1. The patterns of FA and BS show a high content of crystalline phase evidenced by the presence of quartz (ICSD: 062404), Mullite (ICSD: 100805) and Hematite (ICSD: 082137). The presence of an amorphous halo, located in the region 2θ = 18°-30°, corresponds to the glassy phase of the samples. The latter is more pronounced in FA, which may indicate a greater reactivity during the geopolymerization process. The OPC diffractogram shows the main constituents of cement such as tricalcium silicate (C_3S, ICDS: 8110), dicalcium silicate (C_2S, ICDS: 81095), tricalcium aluminate (AC_3, ICDS: 1841) and gypsum (ICDS: 2057); Calcite (ICDS: 73446) is also present as it was used as mineral addition in the OPC production.

Design of experiments

The experimental design was based on RSM, both for the geopolymers synthesized from FA and from BS, in view of finding the optimal molar ratio between SiO_2/Al_2O_3 and Na_2O/SiO_2 and obtaining the blend with the highest response variable regarding the compression strength (MPa). Table 2 presents the factors and levels analyzed for each system FA and BS; thirteen (13) treatments were designed of which four (4) correspond to replications of the central treatment. It should be noted that the levels of the factor SiO_2/Al_2O_3 were selected from the initial molar ratio of each raw material, 3.3 for BS and 4.3 for FA. The compressive strength was tested after 28 days of curing. The linear model or mathematical expression used to process the data is determined by the response surface equation (Eq.1).

$$Y = \beta_0 + \beta_1 X_1 + \beta_2 X_2 + \beta_3 X_1^{\ 2} + \beta_4 X_2^{\ 2} + \beta_5 X_1 X_2 + \varepsilon \quad \text{(Eq. 1)}$$

Where: Y is the response variable 28-day compression strength (MPa); βi are the coefficients of the model, with i=1, 2, 3, 4, 5; X_1 is the molar ratio SiO_2/Al_2O_3; X_2 is the molar ratio Na_2O/SiO_2; and are the quadratic effects; and X_1X_2 is the interaction effect between the molar ratios; finally e is the experimental error. Once the statistical analysis of the response surface model done (Table 2), the results were reviewed and the optimal BS-geo and FA-geo blends were selected and used to synthesize the hybrid materials, the design factors SiO_2/Al_2O_3 and Na_2O/SiO_2 were kept constant and FA/BS were partially substituted by OPC (between 10 and 30%). The optimization process took account of two aspects: the mechanical strength and the potential environmental impacts.

Geopolymer and hybrid systems preparation

Simple 100% FA and 100% BS geopolymer systems were prepared as well as hybrid systems resulting from the mix of FA and BS with OPC at different substitution percentage such as 10, 20 and 30%. A waterglass solution, consisting of commercial sodium silicate (SiO_2 = 32.09%, Na_2O = 11.92%, H_2O = 55.99%) and sodium hydroxide (NaOH 99%, AR grade, Merck) was used as alkaline activator. The ratio liquid/solid (L/S) for the systems 100%FA (FA-geo) and hybrid (HFA), and 100% BS (BS-geo) and hybrid (HBS) was 0.35 and 0.28 respectively. This ratio is calculated assuming that the precursor materials with the sodium hydroxide and the anhydrous sodium silicate constitute the solid mass and the water in the sodium silicate and the mixing water required to obtain the desired handling of the material constitute the liquid mass. Due to the nature of the precursors, the curing temperature conditions were different for each system (BS-Geo, 75°C, 24h+dried at 105°C; FA-Geo and HBS, 75°C; and HFA, 25°C) but all were maintain under > 90% of relative humidity (R.H).

Figure 1. *Physical appearance, SEM micrographs of raw material a) BS, b) FA; and XRD patterns (1= Quartz, 2=Mullite, 3= Hematite, 4= C3S, 5=C2S, 6= C3A, 7=Gypsum, 8=Calcite) (Source: Self-Elaboration)*

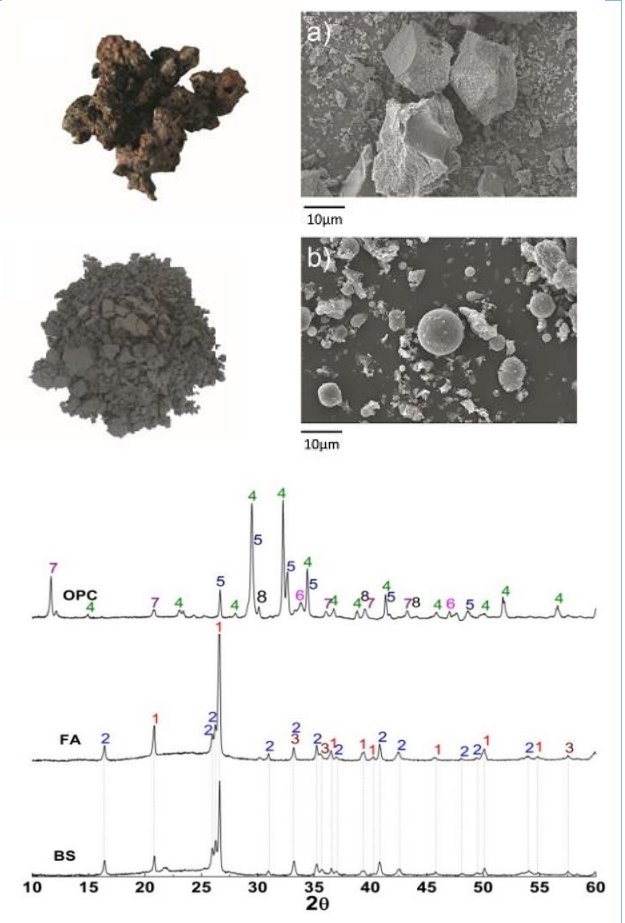

Table 2. *Factors and levels studied (Source: Self-Elaboration)*

System	*Factors*	*Levels*	*Central Points*
FA-geo	SiO_2/Al_2O_3	[4.3] - [6.0]	[5.3]
	Na_2O/SiO_2	[0.2] - [0.3]	[0.25]
BS-geo	SiO_2/Al_2O_3	[3.4] - [4.0]	[3.7]
	Na_2O/SiO_2	[0.2] - [0.3]	[0.25]

Tests and instrumental techniques

Three samples of each formulation, the reference samples (BS-geo and FA-geo) and their respective hybrids (HBS and HFA), were measured for compressive strength at 28 and 90 days of curing, using the universal testing machine INSTRON 3369 at a displacement speed of 1 mm/min. In order to evaluate the performance characteristics of the produced materials, the chloride permeability and the electrical resistivity were tested. The resistance to the penetration of chloride ions was measured following the ASTM C1202 (Standard Test Method for Electrical Indication of Concrete's ability to resist Chloride Penetration) as the charge in Coulombs (C) passed through the material under the application of an external electrical field (60V) during a period of six hours. The test was carried out on cylindrical specimens of 50 mm thick after 28 days of curing. This test, called rapid chloride permeability test (RCPT), is essentially a measurement of electrical conductivity, which depends on both the pore structure, and the chemistry of pore solution.

The microstructural characterization of the samples was carried out using the following techniques:

- Scanning electron microscope (SEM), using a JEOL JSM-6490LV microscope under a high vacuum ($3x10^{-6}$ torr), fitted with an OXFORD INTRUMENTS 7573 INCA PentaFETx3 detector. The samples were gold-sputtered with a Denton VacuumDesk IV unit in order to increase the resolution of the microphotographs.
- X-ray diffraction (XRD), conducted on a PanAnalytical X´Pert MRD diffractometer using a K∝ radiation, a copper X-ray tube, in a range 2θ of 5 to 60°.
- Fourier Transform Infrared Spectroscopy (FTIR) as a supplemental technique to X-ray diffraction. FTIR spectra were obtained on a Perkin Elmer spectrometer model 100 IR, operating in transmission mode, over the range 400 – 2.500 cm^{-1}. Specimens were given a tablet form and mixed with KBr previously dried.

Results and discussion

Geopolymer systems, FA-geo and BS-geo. Optimization of the compressive strength.

The method of least squares was used for the analysis of the results RSM of the systems FA-geo and BS-geo (Table 2) and to determine the estimated parameters both of the interaction model between SiO_2/Al_2O_3 and Na_2O/SiO_2 applied to the fly ash experiment and of the quadratic model of the boiler slag $(Na_2O/SiO_2)^2$. These two models presented satisfactory R^2 values of 93.88% and 90.31% respectively. The proposed mathematical expression for predicting the compressive strength (Rc) in each case is presented in the following equations (Eq. 2, Eq. 3).

$$\mathbf{FA-geo:}\quad Rc = -169.72 + 40.29\,X1 + 501.44\,X2 - 118\,(X1)(X2) + \hat{\varepsilon} \qquad (\mathbf{Eq.2})$$

$$\mathbf{BS-geo:}\quad Rc = 749.36 - 65.61\,X1 - 4316.78\,X2 + 97646\,(X2)\,(X2) + \hat{\varepsilon} \qquad (\mathbf{Eq.3})$$

Based on the variance analysis (Table 3), it can be observed that with a statistical significance of 53.1% for FA-geo and 18.9% for BS-geo, the model fits the data properly (i.e. the lack of fit is not significant). The linear, quadratic and interaction effect hypothesis are considered to be significant if the significance level is less than 5%. The optimal test conditions (X_1 and X_2) for obtaining the maximum compressive strength (Rc) after 28 days curing were analyzed based on the equations (Eq. 2 and Eq. 3) for predicting the compressive strength. To this end, the utility function (D) was used, with values ranging from zero (0) to one (1); 0 indicates that the answer is outside the accepted limits and 1 corresponds to the maximum value. Table 4 shows the different local solutions of the compressive strength optimization.

Figure 2a indicates that to obtain a compressive strength greater than 24 MPa, in the case of the FA-based geopolymers, the following ratios are needed: SiO_2/Al_2O_3 approximately ≥5.70 and a low Na_2O/SiO_2 of approximately ≤0.22. In this case, there is a strong influence of the SiO_2/Al_2O_3 ratio on the mechanical strength. By contrast, in the case of the BS-based geopolymers presented in Figure 2b,

the compressive strength is mainly determined by the Na_2O/SiO_2 ratio, given that the maximum resistance is obtained with low SiO_2/Al_2O_3 and high Na_2O/SiO_2 ratios. However, in order to carry out a comparative study between the production of FA and BS based hybrid materials, the following molar ratios were selected: SiO_2/Al_2O_3 = 3.7 and Na_2O/SiO_2 = 0.25. After 28 days curing, the BS-geo system had a compressive strength of 22 MPa.

Table 3. *Variance analysis for compressive strength at 28 days (Source: Self-Elaboration)*

Factors	*Degrees of freedom*	*Fly ash (FA)*			*Boiler slag (BS)*		
		Sum of squares SC	*F*	*Significance level p- Value*	*Sum of squares SC*	*F*	*Significance level p-Value*
Regression	3	528.34	40.89	0.000	6027.2	24.84	0.000
Linear	2	493.53	61.08	0.000	4887.1	14.42	0.002
SiO_2/Al_2O_3	1	339.86	14.88	0.005	2260.1	15.23	0.005
Na_2O/SiO_2	1	153.67	5.15	0.050	2627.0	11.13	0.010
Interaction							
Si/Al*Na/Si	1	34.81	8.08	0.022			
Na/Si*Na/Si	1				1140.1	14.10	0.006
Residual	8	34.46			647.0		
Lack of fit	4	16.52	0.92	0.531	466.8	2.59	0.189
Error	4	17.94			180.2		
TOTAL	11	562.8			6674.1		

Table 4. *Compressive strength optimization of FA and BS geopolymers (Source: Self-Elaboration)*

System	Compressive strength (CS)	Maximum CS, experimental factors combination	Prediction (CS; D)
FA-geo	Minimum value: 10 MPa Target value: 24 MPa	SiO_2/Al_2O_3: 6.0; Na_2O/SiO_2: 0.2	30.85 MPa; D=1.0
BS-geo	Minimum value: 16 MPa Target value: 60 MPa	SiO_2/Al_2O_3: 3.4; Na_2O/SiO_2: 0.3	107.45 MPa; D=1.0)

Hybrid Systems, HFA and HBS. Optimization of the compressive strength.

Figure 3 presents the compressive strength of the systems HBS and HFA at 28 days of curing. In both cases, the compressive strength increases with the substitution of BS or FA with OPC; however, the results differ depending on the type of precursor used. The BS+30% OPC binders (HBS30) reported a compressive strength of 33.3 MPa, whereas the FA+30% OPC (HFA30) was of 63.6 MPa representing an increase of approximately three (3) times compared to the system FA-geo. From each hybrid material, HBS and HFA, was selected an optimum system for being analyzed by FTIR, XRD and chloride permeability/ electrical resistivity. HBS30 and HFA20 were chosen according on the strength behavior, the target was set at minimum strength of 30 MPa; for instance, HBS30 achieved the target using 30% of OPC, instead HFA20 achieved higher strength than HBS30 using less amount of OPC (20%). The addition of the calcium source in this case OPC in the geopolymer systems regardless of the proportion incorporated accelerates the setting time and hardening of the materials, modifying the curing method of the hybrid materials as was explained previously. The HFA blends do not require a thermal curing; the HBS blends do not need to be dried at 105°C.

The compressive strength development of the hybrid systems specimens up to 90 days of curing is shown in Figure 3b. The plotted bars represent the mean of three tests. It is noted that HBS30 systems presented similar compressive strength at all ages, 40 MPa approximately. On the contrary, the compressive strength of the HFA20 system increases up to two times at 90 days of curing compared with that at 7 days. This same system reaches values of 85.5 MPa at 360 days. In general, the results obtained can be considered in the range of high strength materials.

The results of chloride permeability and electrical resistivity of the geopolymeric and hybrid systems are illustrated in Table 5. FA-Geo and HBS30 system display a total charge passed value < 2000 coulombs and < 1000 coulombs, which is defined according to the classifications of the testing method (ASTM C1202) as corresponding to a low and very low permeability to chlorides respectively. On the contrary, HFA20 shows a higher charge passed, representing (under the assumptions of the test) moderate permeability to chlorides. Generally states that a concrete with RCPT 2000 coulombs charge passed below shows consistently good chloride resistance. Electrical resistivity is an indication of the ingress of aggressive substances in the concrete and it is considered as one of the most significant parameters controlling the rate of active corrosion of the embedded steel reinforcement. That is, a higher resistivity lower movement of electrical charges (ions of concrete pores). From the results reported in Table 5, the hybrid material with higher electrical resistivity was HBS30, ten times higher than HFA20.

Figure 2. *Contour graph. a) FA-geo y b) BS-geo (Source: Self-Elaboration)*

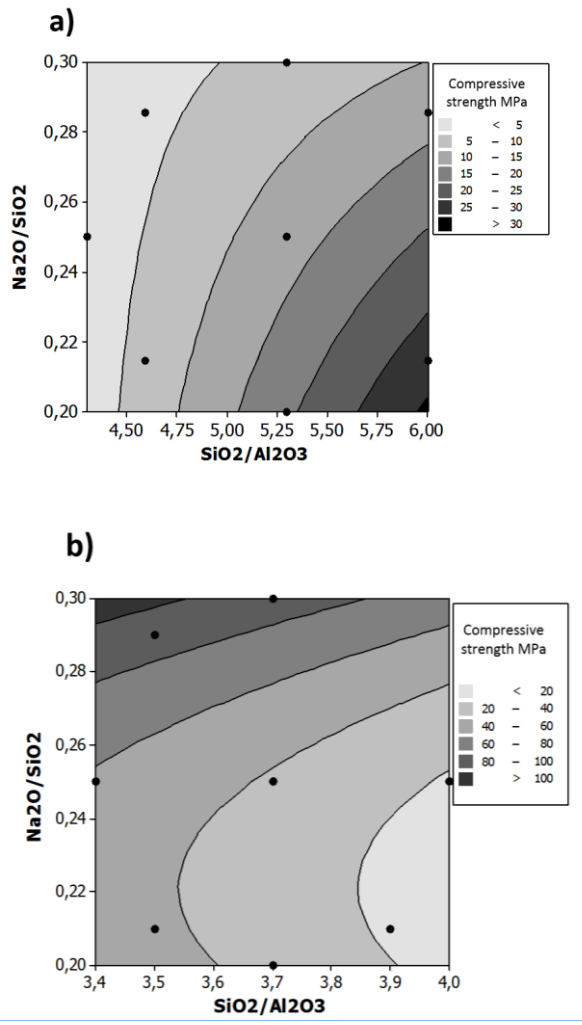

Microstructural Evaluation

The increased mechanical strength of the hybrid system compared to the geopolymer is due to the generation of a larger quantity of binding gel that densifies the matrix as shown in the microphotographs presented in Figure 4a and Figure 4b. The elemental analysis with EDS of the zones selected in this Figure shows the presence of elements such as Na, Ca, Si, O and Al (Table 6); this is indicative of the presence of the two types of gels, the aluminosilicate hydrate N-A-S-H gel and the calcium silicate hydrate C-(A)-S-H gel (García- Lodeiro et al., 2010; 2011; 2013). The existence and equilibrium of both products is possible due to the ion exchange capacity of the alkaline aluminosilicate gel, where the Ca++ ions coming from the OPC displace the Na+ ions from the structure; it is estimated that the Ca++ ions can replace between 67% and 100% of the present Na+ ions. However, the quantity of Ca++ is insufficient to degrade the gel N-A-S-H into a gel C-A-S-H, leading to the formation of a hybrid (N,C)-A-S-H gel (García-Lodeiro et al., 2013) . Another important factor for the stability of the hybrid gel is the pH of the system, which should range between 9 and 12 approximately (García-Lodeiro, 2011).

Figure 5 presents the diffractograms of the systems BS and FA. These show that the crystalline phases of the original materials - given their low or absent reactivity - are not affected by the alkaline attack (García-Lodeiro et al., 2011). Crystalline phases of sodium aluminosilicates such as Gmelinite ($Na_4(Si_8Al_4)O_{24}$•$11H_2O$ ICSD: 069223) and Analcite ($NaAlSi_2O_6$•H_2O, ICSD :2930) are also identified, confirming the presence of a N-A-S-H type binding gel, which is characteristic of the synthesized geopolymers. Similarly, the presence of carbonates like trona ($Na_3H(CO_3)_2$•$2H_2O$, ICSD: 062200) in FA-geo and sodium carbonate ($Na_2(CO_3)$) in BS-geo is also evidenced.

Figure 3. *(a) Compressive strength at 28 days: HFA and HBS system; b) Compressive strength development of hybrid systems (Source: Self-Elaboration)*

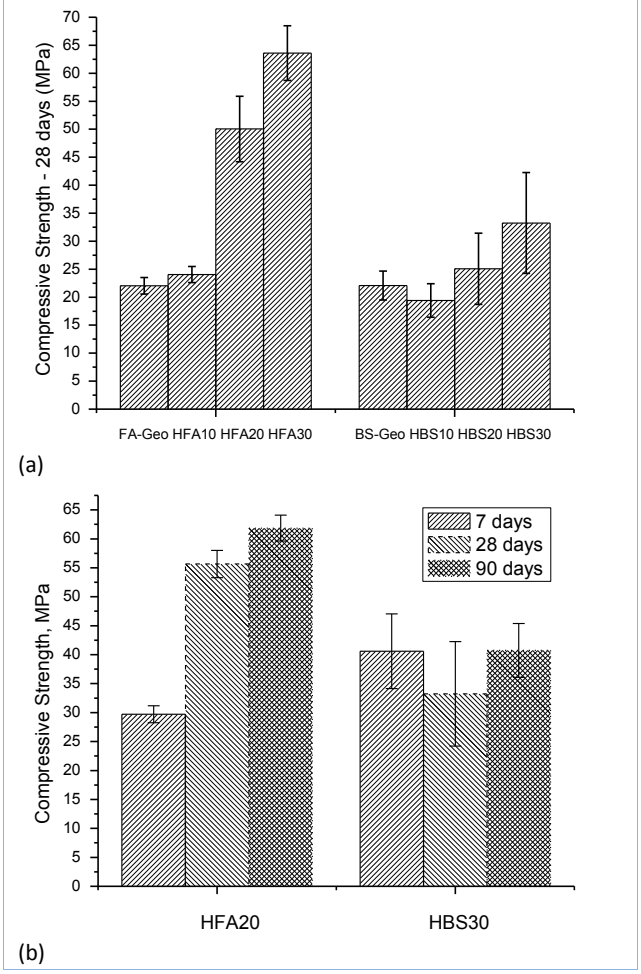

Table 5. *Chloride Permeability and Electrical Resistivity at 28 days of curing (Source: Self-Elaboration)*

System	*Chloride Permeability coulombs*	*Electrical Resistivity Ohm-m*
FA-geo	1478	15.8
HFA20	2877	10.3
HBS30	963	122.0

BS = Boiler slag, FA = Fly ash, H = Hybrid.

The XRD spectra for the hybrid systems HBS30 and HFA20 (Figure 5) show the presence of sodium and/or calcium as pirssonite ($Na_2Ca(CO_3)_2$•$2H_2O$ (ICSD: 9012) and calcite ($CaCO_3$) (ICSD: 080869); sodium carbonates (Na_2CO_3) (ICSD: 006293); calcium silicates (C_3S, C_2S) from the OPC that did not react during the synthesis process are also detected. Portlandite does not appear in the systems. This suggests that the hydration of OPC slackens in the hybrid binder due to the high alkalinity of the system. This condition prevents the precipitation of $Ca(OH)_2$ and, quite likely, leads to the inclusion of the Ca^{2+} ions in the structure of the N-A-S-H gel,

displacing the Na+ ions and causing the formation of the (N,C)-A-S-H and C-A-S-H gels (García-Lodeiro et al., 2010).

Figure 4. *SEM micrographs of hybrid cements. a) HBS30, b) HFA20 (Source: Self-Elaboration)*

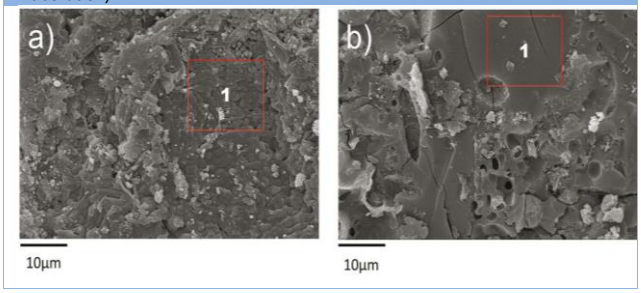

Table 6. *Elemental composition EDS (Source: Self-Elaboration)*

Systems	Element (Zone 1)					
	O	Na	Ca	Si	Al	C
HBS30	32.3	11.5	18.58	15.2	3.8	18.3
HFA20	23.5	6.27	10.91	32.5	3.8	23.1

Figure 5. *XRD patterns. a) BS systems, b) FA systems (1=Quartz, 2=Mullite, 3=Hematite, 4=C3S, 5=C2S, 8=sodium carbonate, 9=Calcite, 10=Pirssonite, 11=Gmelinite, 12=Analcite, 13=Trona) (Source: Self-Elaboration)*

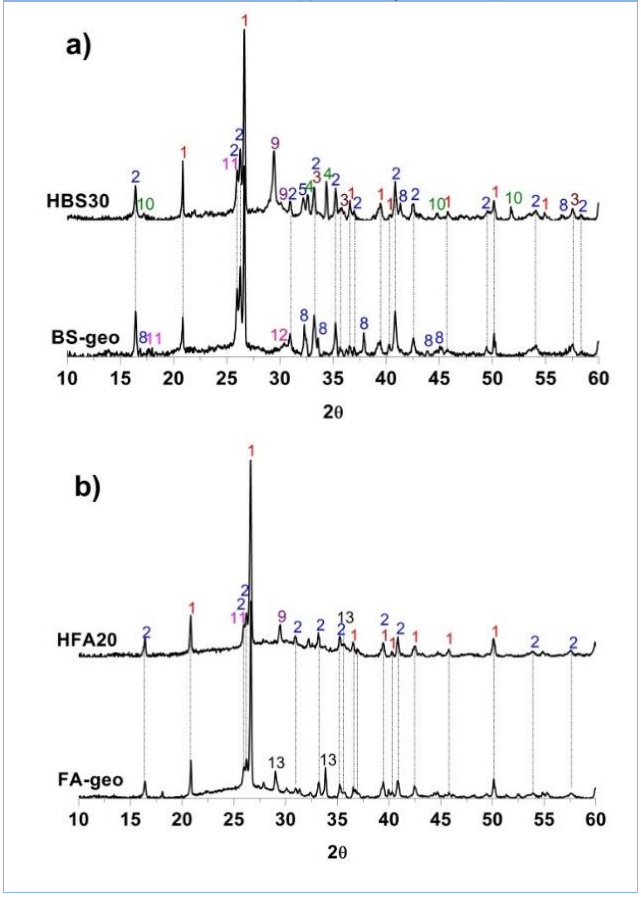

Figure 6 presents the FTIR spectra for the various raw materials used and the geopolymer and hybrid systems synthesized. The fly ash (FA) and the boiler slag (BS) show a main band at around ~1090 cm-1, generated by the T-O-T bond asymmetric stretching vibrations (T=Si, Al) (Rees et al., 2007). The position of the band shifts towards lower frequencies for the geopolymers (BS-geo ~1013 cm^{-1} and FA-geo ~1020 cm^{-1}) (Fernández-Jimenez & Palomo, 2005). This shift is associated with the formation of the sodium aluminosilicate hydrate (N-A-S-H) gel, which consists of a tectosilicate structure with Q4 units formed by silica tetrahedra partially replaced by alumina (Criado et al., 2007; Gadsden, 1975). The band position of the hybrid systems shifts even more (~ 1003-1012 cm^{-1}), which evidences the formation of new products with a lesser degree of polymerization (NASH/CSH/CASH).

In the systems FA-geo, the band is less deep and wider than in the hybrid system HFA20; this is associated with a lesser quantity of hydrate gels and a greater amorphicity. By contrast, the spectra for BS-geo and HBS30 are very similar, which is consistent with the compressive strengths reported. The C-S-H/C-A-S-H gel presents a completely different structure from the N-A-S-H gel; it consists of Q2 silica tetrahedral units partially substituted by aluminum arranged in layers and it is associated to bands located at ~970 cm^{-1} in both hybrid materials (Palomo et al., 2007; García-Lodeiro et al, 2009). The coexistence of both gels in the hybrid sample is linked to its increased compressive strength in comparison with the simple geopolymer (FA-geo and BS-geo).

The FTIR spectra for the geopolymer and hybrid systems confirm the XRD results regarding the presence of sodium and calcium carbonates. The O-C-O bond asymmetric tension band of the CO_3^{-2} functional group is located at ~1410 cm^{-1} at ~1490 cm^{-1}. The band at ~873 cm^{-1} corresponds to the asymmetric stretching vibration of C-O-C bond deformation (García-Lodeiro et al., 2009; Kovalchuk et al., 2008). These bands are also visible in the anhydrous OPC spectrum. It is worth noting that the formation of carbonates takes place through the contact of the atmospheric CO_2 with the hydroxides of alkali metals and alkali-earth metals such as sodium and calcium, present either in the raw material or in the activating solution (Kovalchuk et al., 2008). These bands are particularly pronounced in the OPC spectrum due to presence of the calcium carbonate used as filler. The band situated at ~1650 cm^{-1} corresponds to the H-O-H bond deformation vibration and to the molecular water present in the structure in a superficial way (Gao et al., 2014; Andini et al., 2008). It should be noted that this band is more marked in the hybrid systems, indicating that this type of material produces a larger quantity of hydration products than geopolymers.

Conclusions

Based on the findings of the present study it can be concluded that:

- It is possible to produce geopolymers and hybrid materials from coal combustion wastes, boiler slags and fly ashes (BS and FA) with high contents of unburned material.

- The highest compressive strength is obtained with the following optimal ratios: FA samples, SiO_2/Al_2O_3 = 6 and Na_2O/SiO_2 = 0.2; BS samples, SiO_2/Al_2O_3 = 3.4 and Na_2O/SiO_2 = 0.3. The geopolymers synthesized from BS reach a compressive strength at 28 days of curing of up to 100 MPa, whereas the FA-geopolymers reach 30 MPa. Both cases require heat curing and the first requires an additional drying at 105°C.

- The addition of OPC to the geopolymer systems (FA-geo and BS-geo with the same initial compressive strength, 22

MPa) contributes to increasing the compressive strength as the structures present a higher densification; there is an additional advantage in the case of FA, as no thermal curing is needed. The compressive strength at 28 days of curing of the FA - 20% OPC hybrid system is of approximately 63 MPa and its chloride permeability is moderate. BS – 30% OPC hybrid system reported 40.7 MPa and a low permeability.

- FTIR and DRX confirm the presence of a N-A-S-H type binding gel, which is characteristic of the synthesized geopolymers, and the coexistence of both gels in the hybrid sample; this is related to its increased compressive strength in comparison with the simple geopolymer (FA-geo and BS-geo).

Acknowledgements

The authors wish to thank the Universidad del Valle (Cali, Colombia), Center of Excellence for Novel Materials and the Science, Technology and Innovation Department "COLCIENCIAS" for the support provided throughout this study.

References

Andini, S., Cioffi, R., Colangelo, F., Grieco, T., Montagnaro, F., & Santoro, L. (2008). Coal fly ash as raw material for the manufacture of geopolymer-based products. Waste Manag., 28(2), 416-423. doi:10.1016/j.wasman.2007.02.001

Cabrera-Fuentes, B., Fernandez-Jimenez, A., & Palomo, A. (2011). Alkaline activation of blended fly ash and cement kiln dust, in 13th International Congress on the Chemistry of Cement, Madrid.

Criado, M., Fernández-Jiménez, A., & Palomo, A. (2007). Alkali activation of fly ash: Effect of the SiO2/Na2O ratio. Part I: FTIR study. Microporous Mesoporous Mater., 106(1-3), 180–191. doi:10.1016/j.micromeso.2007.02.055

Damtoft, J.S., Lukasik, J., Herfort, D., Sorrentino, D., & Gartner, E.M. (2008). Sustainable development and climate change initiatives. Cem. Concr. Res., 38(2), 115–127. doi:10.1016/j.cemconres.2007.09.008

Diaz, J., Izquierdo, S., Mejia de Gutierrez, R., & Gordillo, M. (2013). Mezcla ternaria de cemento portland, escoria de alto horno y piedra caliza: resistencia mecánica y durabilidad. Revista de la Construcción, 12(3), 53-60. doi: 10.4067/S0718-915X2013000300006.

Fernández-Jiménez, A., & Palomo, A. (2005). Mid-infrared spectroscopic studies of alkali-activated fly ash structure. Microporous Mesoporous Mater., 86(1–3), 207-214. doi:10.1016/j.micromeso.2005.05.057

Fernández-Jiménez, A., Sobrados, I., & Palomo, A. (2011). Hybrid cements wih very low OPC content, in 13th International Congress on the Chemistry of Cement.

Gadsden, J. A. (1975). Infrared spectra of minerals and related inorganic compounds. Butterworth & Co Publishers Ltd: London.

Gao, K., Lin, K., Wang, D., Hwang, C., Shiu, H., & Chang, Y. (2014). Effects SiO2 / Na2O molar ratio on mechanical properties and the microstructure of nano-SiO2 metakaolin-based geopolymers. Constr. Build. Mater., 53, 503–510. doi: 10.1016/j.conbuildmat.2013.12.003.

García-Lodeiro, I., Fernández-Jiménez, A., & Palomo, A. (2013). Hydration kinetics in hybrid binders: Early reaction stages. Cem. Concr. Compos., 39, 82–92. doi: 10.1016/j.cemconcomp.2013.03.025

García-Lodeiro, I., Fernández-Jiménez, A., Palomo, A. (2013). Variation in hybrid cements over time. Alkaline activation of fly ash–portland cement blends. Cem. Concr. Res., 52, 112–122. doi: 10.1016/j.cemconres.2013.03.022

García-Lodeiro, I., Fernández-Jiménez, A., Palomo, A., & Macphee, D. E. (2010). Effect of Calcium Additions on N-A-S-H Cementitious Gels. J. Am. Ceram. Soc., 93(7), 1934-1940. doi: 10.1111/j.1551-2916.2010.03668.x

García-Lodeiro, I., Macphee, D. E., Palomo, A., & Fernández-Jiménez, A. (2009). Effect of alkalis on fresh C–S–H gels. FTIR analysis. Cem. Concr. Res., 39(3), 147-153. doi: 10.1016/j.cemconres.2009.01.003

Garcia-Lodeiro, I., Palomo, A., Fernández-Jiménez, A., & Macphee, D. E. (2011). Compatibility studies between N-A-S-H and C-A-S-H gels. Study in the ternary diagram Na2O–CaO–Al2O3–SiO2–H2O. Cem. Concr. Res., 41(9), 923–931. doi: 10.1016/j.cemconres.2011.05.006

Imbabi, M. S., Carrigan, C., & McKenna, S. (2012). Trends and developments in green cement and concrete technology. Int. J. Sustain. Built Environment, 1(2), 194–216. doi: 10.1016/j.ijsbe.2013.05.001

Kovalchuk, G., Palomo, A., & Fernández-Jiménez, A., (2008). Alkali-activated fly ash . Relationship between mechanical strength gains and initial ash chemistry. Mater. Construcción, 58, 35–52. http://digital.csic.es/bitstream/10261/8092/3/140.pdf

Lothenbach, B., Scrivener, K., & Hooton, R.D. (2011). Supplementary cementitious materials. Cem. Concr. Res., 41(12), 1244-1256. doi:10.1016/j.cemconres.2010.12.001

Macphee, D., & Garcia-Lodeiro, I. (2011). Activation of aluminosilicates - some chemical considerations, in Slag Valorisation Symposium, pp. 51–61.

OMM (2013) Boletin sobre los gases de efecto invernadero, Reporte N°9, Noviembre 6 de 2013. [Online]. Retrieved from: http://www.wmo.int/pages/prog/arep/gaw/ghg/documents/GHG_Bulletin_No.9_es.pdf [visited 29.11.2014]

Palomo, A., Fernández-Jiménez, A., Kovalchuk, G., Ordoñez, L. M., & Naranjo, M. C. (2007). OPC-fly ash cementitious systems: study of gel binders produced during alkaline hydration. J. Mater. Sci., 42(9), 2958-2966. Doi: 10.1007/s10853-006-0585-7

Rees, C. A., Provis, J. L., Lukey, G. C., & van Deventer, J. S. J. (2007). In Situ ATR-FTIR Study of the Early Stages of Fly Ash Geopolymer Gel Formation. Langmuir, 23(17), 9076–9082. doi: 10.1021/la701185g

Robayo, R., Mattey, P., & Delvasto, S. (2013). Comportamiento mecánico de un concreto fluido adicionado con ceniza de cascarilla de arroz (CCA) y reforzado con fibras de acero. Revista de la Construcción, 12(2), 139-151. doi: 10.4067/S0718-915X2013000200011.

Schneider, M., Romer, M., Tschudin, M., & Bolio, H. (2011). Sustainable cement production-present and future. Cem. Concr. Res., 41(7), 642-650. doi:10.1016/j.cemconres.2011.03.019

Shi, C., Fernández-Jiménez, A., & Palomo, A. (2011). New cements for the 21st century: The pursuit of an alternative to Portland cement. Cem. Concr. Res., 41(7), 750–763. doi:10.1016/j.cemconres.2011.03.016

Van Oss, H. G. (2014). U.S. Geological Survey, Mineral Commodity Summaries. [Online]. Retrieved from: http://minerals.usgs.gov/minerals/pubs/commodity/cement/mcs-2014-cemen.pdf [visited 29.11.2014]

Yoon, S., Monteiro, P. J. M., Macphee, D. E., Glasser, F. P., & Imbabi, M. S. E. (2014). Statistical evaluation of the mechanical properties of high-volume class F fly ash concretes. Constr. Build. Mater., 54, 432-442. doi: 10.1016/j.conbuildmat.2013.12.077

Figure 6. *IR spectra. a) Raw material, b) BS system, c) FA syste. (Source: Self-Elaboration)*